

Revisiting Kekulene: Synthesis and Single-Molecule Imaging

Iago Pozo,[†] Zsolt Majzik,[‡] Niko Pavliček,[‡] Manuel Melle-Franco,[§] Enrique Guitián,[†] Diego Peña,^{*,†} Leo Gross,[‡] and Dolores Pérez^{*,†}

[†]Centro Singular de Investigación en Química Biolóxica e Materiais Moleculares (CIQUS) and Departamento de Química Orgánica, Universidade de Santiago de Compostela, 15782 Santiago de Compostela, Spain

[‡]IBM Research–Zürich, 8803 Rüschlikon, Switzerland

[§]CICECO, Aveiro Institute of Materials, Department of Chemistry, University of Aveiro, 3810-193 Aveiro, Portugal

Supporting Information

ABSTRACT: Four decades after the first (and only) reported synthesis of kekulene, this emblematic cycloarene has been obtained again through an improved route involving the construction of a key synthetic intermediate, 5,6,8,9-tetrahydrobenzo[*m*]tetraphene, by means of a double Diels–Alder reaction between styrene and a versatile benzodiyne synthon. Ultra-high-resolution AFM imaging of single molecules of kekulene and computational calculations provide additional support for a molecular structure with a significant degree of bond localization in accordance with the resonance structure predicted by the Clar model.

Cycloarenes¹ constitute a fascinating class of polycyclic aromatic hydrocarbons (PAHs) that have attracted the scientific community for decades due to the singularity of their molecular and electronic structures.² They serve as ideal platforms to investigate fundamental questions around the concept of aromaticity and, in particular, those related with the π -electron distribution in complex aromatic systems.³ Recently, renewed attention to cycloarenes has arisen since they serve as models for graphene pores.⁴ Kekulene (**1**) is probably the best studied member of this family. Its electronic structure has been the subject of debate for decades,⁵ the Clar model **1a** and the annulenoid Kekule structure **1b** being of special interest (Figure 1). In fact, properties such as superaromaticity^{6,7} have been initially attributed to this molecule, associated with hypothetically representative annulenoid structures such as **1b**, comprising two concentric $[4n+2]$ π -electron circuits.

While many theoretical studies on the electronic structure of cycloarenes have been reported, the experimental study of their

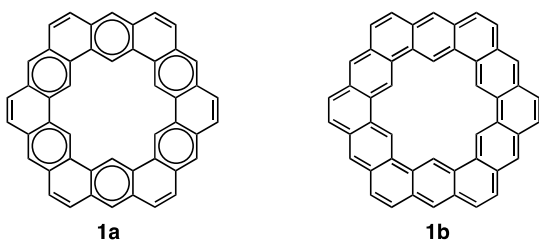
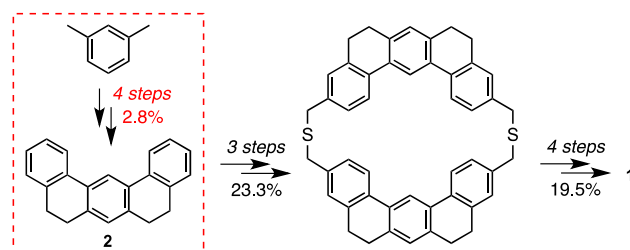


Figure 1. Clar (**1a**) and Kekule annulenoid (**1b**) structures of kekulene.

properties has been limited due to the extremely challenging synthesis of this kind of planar, *cata*-condensed aromatic macrocyclic systems.² In fact, the synthesis and characterization of kekulene by Staab and Diederich in 1978^{1,8} is considered to be a landmark achievement in the field of aromatic chemistry. Only two additional nearly planar, unsubstituted cycloarenes, cyclo[*d,e,d,e,e,d,e,d,e*]-decakisbenzene⁹ and septulene,¹⁰ have been synthesized so far, while substituted analogues of kekulene and of the higher homologue, nonplanar octulene, have been recently accessed taking advantage of their higher solubility.¹¹ However, Staab and Diederich's synthesis of the parent kekulene (Scheme 1) remains unsurpassed, and apparently unrepeated, since the only available experimental studies on **1** are those reported by this group 40 years ago.^{1,8,12}

Scheme 1. Synthetic Approach to Kekulene by Staab and Diederich^{1,8a}



Our expertise and continuing interest in the chemistry of polycyclic aromatic compounds and nanographenes led us to turn our attention to this captivating molecule. Thus, here we present our contribution to the study of kekulene through three different yet related achievements: the improved synthesis of **1** by means of the aryne-mediated construction of a key synthetic intermediate, the single-molecule imaging of this fascinating cycloarene by ultra-high-resolution atomic force microscopy (AFM), and a computational study including the accurate simulation of the experimentally observed AFM images.

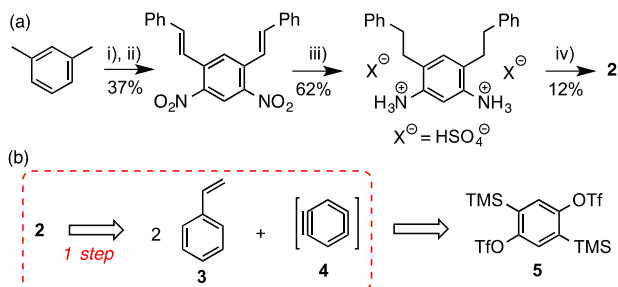
As shown in Scheme 1, probably the main drawback of the otherwise superb synthesis of **1** is the preparation of 5,6,8,9-tetrahydrobenzo[*m*]tetraphene (**2**).¹³ The construction of the

Received: July 24, 2019

Published: September 17, 2019

key synthetic intermediate **2**, far from being straightforward, was reported to occur in four steps, involving relatively harsh reaction conditions and in a poor overall 2.8% yield (Scheme 2a).¹ Our wide experience in the application of bistriflate **5** and

Scheme 2. (a) Staab and Diederich's Synthesis of **2,^a and (b) This Work's Aryne-Based Retrosynthetic Approach to **2****

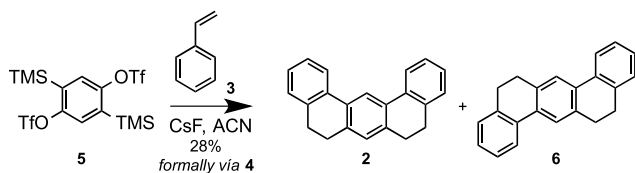


^aConditions: (i) conc. HNO₃, Δ; (ii) PhCHO, piperidine; (iii) H₂, 90 atm, 10% Pd/C, Δ; (iv) Cu, conc. H₂SO₄, isoamyl nitrite.

other bisaryne precursors to the synthesis of diverse PAHs of interest^{14,15} led us to envision an alternative approach to **2** through a double Diels–Alder reaction involving two molecules of styrene (**3**) and the 1,4-benzodiyne synthon **4**, which would be generated by fluoride-induced elimination from bistriflate **5**,¹⁶ which is currently commercially available (Scheme 2b).

The participation of styrenes as unconventional dienes in Diels–Alder cycloadditions with arynes to yield dihydropheanthrenes has been previously reported, although these transformations are commonly complicated by secondary reactions such as aryne-mediated dehydrogenation to give phenanthrenes,¹⁷ or by the concerted ene reaction of the initial Diels–Alder adduct with a second aryne equivalent to afford arylated products.¹⁸ In our case, such a Diels–Alder/ene cascade would be particularly problematic, since the enincorporated aryl moiety would contain *ortho*-disposed trimethylsilyl and triflate functionalities, which are able to generate new aryne species and give rise, probably, to oligomerization processes and complex reaction mixtures. Despite these possible difficulties, we targeted the synthesis of **2** by reaction of styrene with 1,4-bisbenzyne precursor **5** under aryne-forming conditions (Scheme 3, Table 1).

Scheme 3. Reaction of Bistriflate **5 with CsF in the Presence of Styrene**



Initial assays were performed in refluxing dioxane using CsF as the fluoride source, conditions that had been previously reported for the unusual selective preparation of non-arylated 9,10-dihydropheanthrene by reaction of styrene with benzyne.¹⁹ Encouragingly, treatment of **5** with CsF in refluxing dioxane, in the presence of excess **3**, resulted in the formation of the expected products **2** and **6**, although in modest yield

Table 1. Optimization of the Reaction Conditions^a

entry	solvent	molar ratio 5:3:CsF	scale (mmol 5)	yield 2 + 6 (%) ^b
1	dioxane	1:5:10	0.2	17
2 ^c	dioxane	1:5:10	0.2	11
3 ^d	dioxane	1:5:10	0.2	–
4 ^e	ACN	1:5:10	0.2	13
5	ACN	1:5:10	0.2	20
6	ACN	1:2:10	0.2	12
7 ^f	ACN	1:25:10	0.2	23
8	ACN	1:5:6	0.2	20
9	ACN	1:5:6	1.4	22
10	ACN	1:5:6	6	26
11	ACN	1:5:6	19	28

^aTypical reaction conditions: reflux under Ar, 16 h, [**5**] = 0.05 M.

^bYield of isolated product (~2:3 mixture of **2** and **6**). ^c18-crown-6 (120 mol%) was added. ^dTBAF was used as the source of fluoride.

^eReaction conducted at room temperature. ^f[**5**] = 0.01 M.

(entry 1). Addition of 18-crown-6 (entry 2) or the use of TBAF as fluoride source (entry 3) led to poorer results.

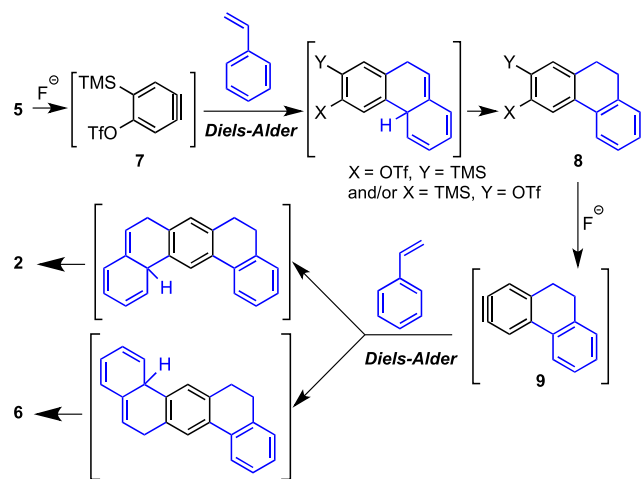
The use of acetonitrile (ACN) as solvent led to slightly better yields (entry 5), and under these conditions, the molar ratio of 5:3:CsF was optimized (entries 5–8). Finally, we proved that better yields were consistently obtained when the reaction was performed on a higher scale (entries 8–11). The best results were obtained by reaction of **5** (19–20 mmol) with styrene (**3**) and CsF (in 1:5:6 molar ratio) in refluxing acetonitrile, yielding a 2:3 mixture of tetrahydrobenzotetraphenes **2** and **6** in a reasonable 28% yield (entry 11). The separation of both isomers was not easy, but it could be achieved by semi-preparative supercritical fluid chromatography (SFC)²⁰ and also by sequential recrystallizations from boiling methanol.

These results can be considered highly remarkable, since compound **2**, a key intermediate in the synthesis of kekulene (**1**), is obtained in just one step from commercially available materials under mild reaction conditions and with a 4-fold increased yield with respect to that of the previously reported synthesis.

Remarkably, the only isolable compounds detected in the crude reaction mixtures were **2**, **6**, and excess styrene (**3**).²⁰ Products derived either from dehydrogenation of **2/6** or from Diels–Alder/ene cascade processes were not observed.²¹ However, the formation of insoluble oligomers or polymers derived from aryne-based side reactions cannot be ruled out. The mechanism proposed for the formation of **2** (and **6**) involves two probably sequential Diels–Alder/H-migration processes. The detection of the functionalized dihydropheanthrene **8** in some experiments strongly suggests that the first Diels–Alder reaction of styrene with monoaryne **7** and the subsequent H-migration occur prior to the generation of the second aryne insaturation in **9** (Scheme 4). Once compound **2** was conveniently prepared, we proceeded to complete the synthesis of kekulene (**1**). After attempting some new synthetic alternatives based on metal-catalyzed couplings and/or olefin metathesis/isomerization reactions, we decided to rely on the firmly established route described by Diederich and Staab,^{1,8} which in our hands was perfectly reproducible, even under significantly lower scale conditions.

With kekulene (**1**) in hand, we identified the opportunity to visualize its molecular structure by ultra-high-resolution AFM,²² a state-of-the-art technique for the single-molecule

Scheme 4. Mechanistic Proposal for the Formation of 2/6



study of planar, conjugated systems. As recently demonstrated, this technique, in combination with scanning tunneling microscopy (STM), has become a powerful tool for the elucidation and study of individual molecules.²³ In order to increase the sublimation rate with respect to the fragmentation rate, the material was sublimated by rapid heating^{24a} from a Si wafer^{24b} onto a Cu(111) substrate, holding the sample at $T = 10$ K during deposition. The large size and thus high sublimation temperature of kekulene were expected to result in fragmentation, and, in fact, the preparation resulted mostly in small and often mobile molecules on the surface. However, we found a few molecules of the expected hexagonal shape and size of kekulene. Constant-height AFM images of the molecule adsorbed on Cu(111) with a CO-functionalized tip^{22,25–28} were recorded at different heights (Figure 2), with decreasing tip-to-sample distance in Figure 2a–c. Corresponding Laplace-filtered images are shown in Figure 2d–f, respectively. From the AFM images, the molecular structure of kekulene (1) was resolved. In addition, details of the contrast can be related to

bond order. Resolving the bond-order-related contrast is challenging at the periphery of molecules because of the nonplanar background from van der Waals and electrostatic forces.^{27,29} However, bonds that experience similar background forces are comparable, allowing qualitative resolution of bond-order differences. Increased bond order results in brighter appearance at moderate tip heights and shortened appearance of bonds at small tip heights.²⁷ In the case of kekulene (1), the peripheral C(H)–C(H) bonds appear as the overall brightest bonds at moderate tip height, i.e., in Figure 2a,b, and as the shortest bonds at small tip height, i.e., in Figure 2c. Both observations indicate that these are the bonds of the highest bond order within the kekulene structure, which is in agreement with previous experimental evidence obtained by X-ray diffraction (XRD) studies of single crystals of 1.^{8b}

To gain further insight into the interpretation of the AFM images in connection with the molecular structure of 1, we computed the kekulene molecule both in the gas phase and on the Cu(111) surface and performed simulations of AFM images.²⁰ Calculations in the gas phase at the B3LYP-def2-TZVP level³⁰ reveal that the molecule possesses D_{3d} symmetry since the hydrogen atoms of the inner cavity or pore present a slight distortion out of the molecular plane due to steric hindrance. Remarkably, the calculated C–C bond distances reproduce the experimental solid-state XRD values within 0.01 Å (Figure 4). This bonding pattern, which is also reproduced by on-surface calculations, matches perfectly the predictions of the π -sextet rule³¹ and supports the Clar model 1a, with the highest possible number of disjoint aromatic π -sextets (six), as the most representative structure of kekulene. Thus, despite its 48 π electrons ($6n$ π electrons), kekulene is far from being “fully benzenoid”, as the π electrons are not highly delocalized. In fact, 1 possesses an unusually high calculated HOMO–LUMO gap of 3.55 eV (B3LYP-def2-TZVP level), similar to that calculated for the much smaller anthracene molecule (3.56 eV). Finally, simulations of the AFM images were performed with a Molecular Mechanics (MM) model as implemented in the Probe Particle Model (PPM) software.^{20,28,32} We

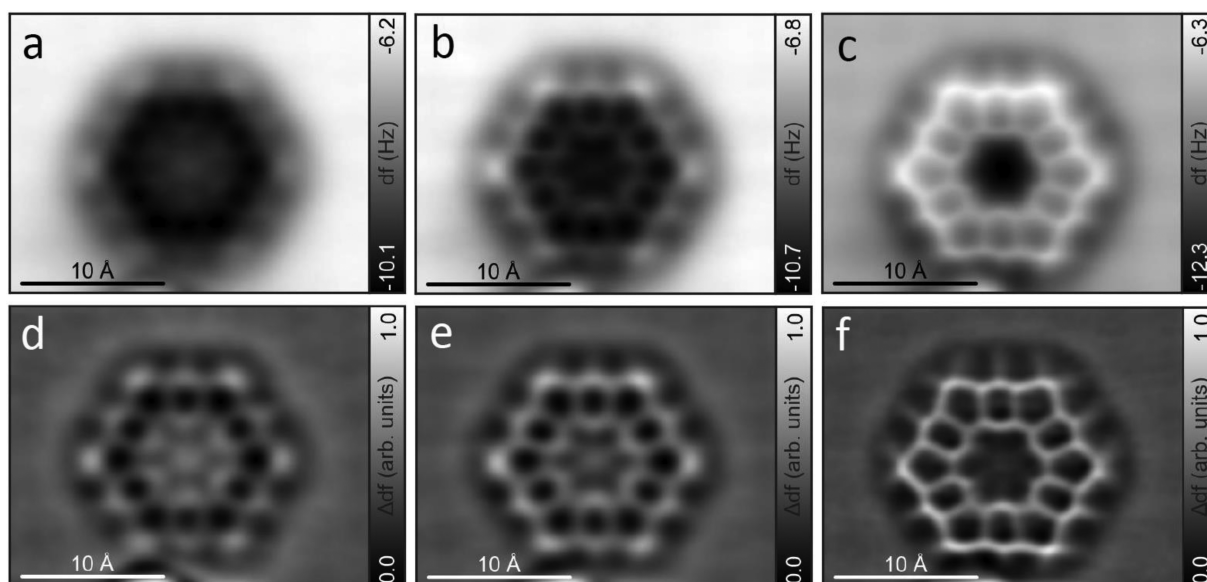


Figure 2. Experimental AFM images of kekulene (1) on Cu(111). (a–c) Constant-height AFM images with a CO-functionalized tip, amplitude $A = 1$ Å, sample voltage $V = 0$ V. We approached the tip by $z = 1.6$ Å in (a), 1.9 Å in (b), and 2.2 Å in (c) with respect to the STM set point of $V = 0.1$ V, $I = 1$ pA on the bare Cu(111) surface. (d–f) Corresponding Laplace-filtered images.

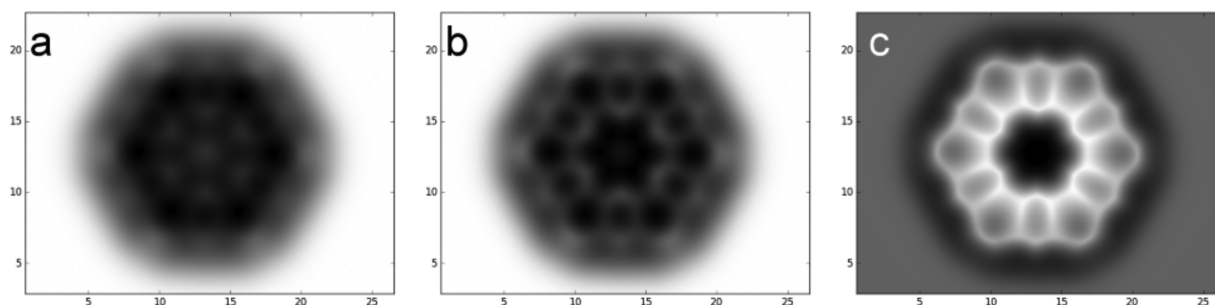


Figure 3. PPM-simulated AFM images with an amplitude of $A = 1 \text{ \AA}$ computed with a PBE QM/MM electrostatic potential interacting with a classical d_z^2 -like quadrupole tip ($Qd_z^2 = -0.25 \text{ e}^-/\text{\AA}^2$) with a bending stiffness of 0.35 N/m at $z = 3.4 \text{ \AA}$ in (a), 3.3 \AA in (b), and 3 \AA in (c) with respect to the molecular plane. All distances are in \AA .

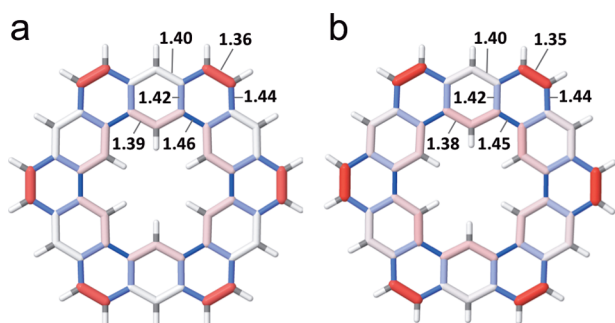


Figure 4. (a) Molecular structure of kekulene (**1**) computed at the B3LYP-def2-TZVP level in vacuum. (b) Experimental structure from XRD, $C2/c$ space group symmetry. The colors grade with distance from 1.33 \AA (red) to 1.40 \AA (white) and to 1.47 \AA (blue). Bond lengths are in \AA .

computed images with an experimental amplitude of 1.0 \AA and with different binding constants, k , ranging from 0.15 to 0.60 N/m , and uncharged, monopole and quadrupole tips. The best match to the experimental images was achieved by a d_z^2 -like quadrupole tip³³ with $Qd_z^2 = -0.25$ and a bending constant of $k = 0.35 \text{ N/m}$ (see Figure 3).³⁴

In conclusion, this work provides a significant contribution to the synthesis of kekulene (**1**) based on the improved preparation of the key intermediate 5,6,8,9-tetrahydrobenzo- $[m]$ tetraphene (**2**) by means of aryne chemistry. The modified protocol has been applied to the actual synthesis of **1**, which, to the best of our knowledge, had not been synthesized nor experimentally studied since the seminal work by Staab and Diederich in the early 1980s. With this material in hand, the structure of individual molecules of kekulene (**1**) was nicely resolved by ultra-high-resolution AFM. The computational study of kekulene (**1**) in vacuum and on the Cu(111) surface and the successful simulation of the experimental single-molecule AFM images provided further evidence of a bonding pattern for kekulene which matches with the molecular structure predicted by Clar's π -sextet rule.

■ ASSOCIATED CONTENT

📄 Supporting Information

The Supporting Information is available free of charge on the ACS Publications website at DOI: [10.1021/jacs.9b07926](https://doi.org/10.1021/jacs.9b07926).

Experimental procedures, synthesis, characterization, AFM imaging, and computational details (PDF)

■ AUTHOR INFORMATION

Corresponding Authors

*diego.pena@usc.es

*dolores.perez@usc.es

ORCID

Zsolt Majzik: 0000-0002-9985-9581

Niko Pavliček: 0000-0003-3989-4454

Diego Peña: 0000-0003-3814-589X

Leo Gross: 0000-0002-5337-4159

Dolores Pérez: 0000-0003-0877-5938

Notes

The authors declare no competing financial interest.

■ ACKNOWLEDGMENTS

Financial support from the Spanish Agencia Estatal de Investigación (CTQ2016-78157-R and MAT2016-78293-C6-3-R; AEI/FEDER, UE), Xunta de Galicia (Centro singular de investigación de Galicia accreditation 2016–2019, ED431G/09), the European Union (European Regional Development Fund-ERDF), and the ERC Consolidator Grant AMSEL (682144) as well as from the Portuguese Foundation for Science and Technology (FCT), under the projects PTDC/FIS-NAN/4662/2014, IF/00894/2015, and CICECO - Aveiro Institute of Materials, FCT ref. UID/CTM/50011/2019, is gratefully acknowledged. I.P. thanks Xunta de Galicia and European Union (European Social Fund, ESF) for the award of a predoctoral fellowship. In addition, M.M.-F. would like to thank the Project HPC-EUROPA3 (INFRAIA-2016-1-730897) and the Barcelona Supercomputing Center for computer resources and technical support. This paper is dedicated to Prof. François Diederich and to the memory of Prof. Heinz A. Staab.

■ REFERENCES

- (1) Staab, H. A.; Diederich, F. Synthesis of Kekulene. *Chem. Ber.* **1983**, *116*, 3487–3503.
- (2) For an excellent recent review, see: Buttrick, J. C.; King, B. T. Kekulenes, Cycloarenes, and Heterocycloarenes: Addressing Electronic Structure and Aromaticity through Experiments and Calculations. *Chem. Soc. Rev.* **2017**, *46*, 7–20.
- (3) (a) Aihara, J. π -Electron Currents Induced in Polycyclic Benzenoid Hydrocarbons and their Relationship to Clar Structures. *J. Phys. Chem. A* **2003**, *107*, 11553–11557. (b) Randić, M. Aromaticity of Polycyclic Conjugated Hydrocarbons. *Chem. Rev.* **2003**, *103*, 3449–3605. (c) Aihara, J.; Makino, M. Constrained Clar Formulas of Coronoid Hydrocarbons. *J. Phys. Chem. A* **2014**, *118*, 1258–1266. (d) Stepien, M. An Aromatic Riddle: Decoupling Annulene Conjugation in Coronoid Macrocycles. *Chem.* **2018**, *4*,

1481–1491. (e) Liu, C.; Ni, Y.; Lu, X.; Li, G.; Wu, J. Global Aromaticity in Macrocyclic Polyradicaloids: Hückel's Rule or Baird's Rule? *Acc. Chem. Res.* **2019**, *52*, 2309–2321.

(4) (a) Robertson, A. W.; Lee, G.-D.; He, K.; Gong, C.; Chen, Q.; Yoon, E.; Kirkland, A. I.; Warner, J. H. Atomic Structure of Graphene Subnanometer Pores. *ACS Nano* **2015**, *9*, 11599–11607. (b) Beser, U.; Kastler, M.; Maghsoumi, A.; Wagner, M.; Castiglioni, C.; Tommasini, M.; Narita, A.; Feng, X.; Müllen, K. A C₂₁₆-Nanographene Molecule with Defined Cavity as Extended Coronoid. *J. Am. Chem. Soc.* **2016**, *138*, 4322–4325. (c) Hieulle, J.; Carbonell-Sanromà, E.; Vilas-Varela, M.; García-Lekue, A.; Guitián, E.; Peña, D.; Pascual, J. I. On-surface Route for Producing Planar Nanographenes with Azulene Moieties. *Nano Lett.* **2018**, *18*, 418–423. (d) Moreno, C.; Vilas-Varela, M.; Kretz, B.; García-Lekue, A.; Costache, M. V.; Paradinas, M.; Panighel, M.; Ceballos, G.; Valenzuela, S. O.; Peña, D.; Mugarza, A. Bottom-up Synthesis of Multifunctional Nanoporous Graphene. *Science* **2018**, *360*, 199–203. (e) Xu, K.; Urgel, J. I.; Eimre, K.; Di Giovannantonio, M.; Keerthi, A.; Komber, H.; Wang, S.; Narita, A.; Berger, R.; Ruffieux, P.; Pignedoli, C. A.; Liu, J.; Müllen, K.; Fasel, R.; Feng, X. On-Surface Synthesis of a Nonplanar Porous Nanographene. *J. Am. Chem. Soc.* **2019**, *141*, 7726–7730.

(5) For seminal contributions, see: (a) McWeeny, R. The Diamagnetic Anisotropy of Large Aromatic Systems: III Structures with Hexagonal Symmetry. *Proc. Phys. Soc., London, Sect. A* **1951**, *64*, 921–930. (b) Aihara, J. On the Number of Aromatic Sextets in a Benzenoid Hydrocarbon. *Bull. Chem. Soc. Jpn.* **1976**, *49*, 1429–14230.

(6) (a) Cioslowski, J.; O'Connor, P. B.; Fleischmann, E. D. Is Superbenzene Superaromatic? *J. Am. Chem. Soc.* **1991**, *113*, 1086–1089. (b) Aihara, J. Is Superaromaticity a Fact or an Artifact? The Kekulene Problem. *J. Am. Chem. Soc.* **1992**, *114*, 865–868. (c) Jiao, H.; Schleyer, P. R. Is Kekulene Really Superaromatic? *Angew. Chem., Int. Ed. Engl.* **1996**, *35*, 2383–2386. (d) Zhou, Z. Are kekulene, coronene, and corannulene tetraanion superaromatic? Theoretical examination using hardness indices. *J. Phys. Org. Chem.* **1995**, *8*, 103–107. (e) Aihara, J.; Makino, M.; Ishida, T.; Dias, J. R. Analytical Study of Superaromaticity in Cycloarenes and Related Coronoid Hydrocarbons. *J. Phys. Chem. A* **2013**, *117*, 4688–4697.

(7) The synthesis of two structurally related macrocyclic polyradicaloids, with “annulene-within-an-annulene” structure and unusual global aromaticity, has been recently reported: Liu, C.; Sandoval-Salinas, M. E.; Hong, Y.; Gopalakrishna, T. Y.; Phan, H.; Aratani, N.; Herng, T. S.; Ding, J.; Yamada, H.; Kim, D.; Casanova, D.; Wu, J. Macrocyclic Polyradicaloids with Unusual Super-ring Structure and Global Aromaticity. *Chem.* **2018**, *4*, 1586–1595.

(8) (a) Diederich, F.; Staab, H. A. Benzenoid versus Annulene Aromaticity: Synthesis and Properties of Kekulene. *Angew. Chem., Int. Ed. Engl.* **1978**, *17*, 372–374. (b) Krieger, C.; Diederich, F.; Schweitzer, D.; Staab, H. A. Molecular Structure and Spectroscopic Properties of Kekulene. *Angew. Chem., Int. Ed. Engl.* **1979**, *18*, 699–701. (c) Staab, H. A.; Diederich, F.; Krieger, C.; Schweitzer, D. Molecular Structure and Spectroscopic Properties of Kekulene. *Chem. Ber.* **1983**, *116*, 3504–3512.

(9) Funhoff, D. J. H.; Staab, H. A. Cyclo[*d.e.d.e.d.e.d.e.*]-decakisbenzene, a New Cycloarene. *Angew. Chem., Int. Ed. Engl.* **1986**, *25*, 742–744.

(10) Kumar, B.; Viboh, R. L.; Bonifacio, M. C.; Thompson, W. B.; Buttrick, J. C.; Westlake, B. C.; Kim, M.-S.; Zoellner, R. W.; Varganov, S. A.; Mörschel, P.; Teteruk, J.; Schmidt, M. U.; King, B. T. Septulene: The Heptagonal Homologue of Kekulene. *Angew. Chem., Int. Ed.* **2012**, *51*, 12795–12800.

(11) Majewski, M. A.; Hong, Y.; Lis, T.; Gregolinski, J.; Chmielewski, P. J.; Cybinska, J.; Kim, D.; Stepien, M. Octulene: A Hyperbolic Molecular Belt that Binds Chloride Anions. *Angew. Chem., Int. Ed.* **2016**, *55*, 14072–14076.

(12) Schweitzer, D.; Hausser, K. H.; Vogler, H.; Diederich, F.; Staab, H. A. Electronic Properties of Kekulene. *Mol. Phys.* **1982**, *46*, 1141–1153.

(13) This specific, partially hydrogenated PAH, is needed to guarantee the conformational flexibility required for the penultimate

step in the synthesis of kekulene (a double photochemical cycloisomerization; see ref 1 for details).

(14) (a) Schuler, B.; Collazos, S.; Gross, L.; Meyer, G.; Pérez, D.; Guitián, E.; Peña, D. From Perylene to a 22-Ring Aromatic Hydrocarbon in One-Pot. *Angew. Chem., Int. Ed.* **2014**, *53*, 9004–9006. (b) Rodríguez-Lojo, D.; Peña, D.; Pérez, D.; Guitián, E. Large Phenyl-Substituted Acenes by Cycloaddition Reactions of the 2,6-Naphthodiyne Synthon. *Chem. Commun.* **2015**, *51*, 5418–5420. (c) Rodríguez-Lojo, D.; Peña, D.; Pérez, D.; Guitián, E. Straightforward Synthesis of Novel Acene-Based Aryne Precursors. *Synlett* **2015**, *26*, 1633–1637. (d) Pozo, I.; Cobas, A.; Peña, D.; Guitián, E.; Pérez, D. 1,7-Naphthodiyne: a New Platform for the Synthesis of Novel, Sterically Congested PAHs. *Chem. Commun.* **2016**, *52*, 5534–5537. (e) García, D.; Rodríguez-Pérez, L.; Herranz, M. A.; Peña, D.; Guitián, E.; Bailey, S.; Al-Galiby, Q.; Noori, M.; Lambert, C. J.; Pérez, D.; Martín, N. A C₆₀-Aryne Building Block: Synthesis of a Hybrid All-Carbon Nanostructure. *Chem. Commun.* **2016**, *52*, 6677–6680. (f) Krüger, J.; García, F.; Eisenhut, F.; Skidin, D.; Alonso, J. M.; Guitián, E.; Pérez, D.; Cuniberti, G.; Moresco, F.; Peña, D. Decacene: On-Surface Generation. *Angew. Chem., Int. Ed.* **2017**, *56*, 11945–11948. (g) Schulz, F.; García, F.; Kaiser, K.; Pérez, D.; Guitián, E.; Gross, L.; Peña, D. Exploring a Route to Cyclic Acenes by On-Surface Synthesis. *Angew. Chem., Int. Ed.* **2019**, *58*, 9038–9042.

(15) For representative examples by other authors, see: (a) Li, J.; Zhao, Y.; Lu, J.; Li, G.; Zhang, J.; Zhao, Y.; Sun, X.; Zhang, Q. Double [4 + 2] Cycloaddition Reaction to Approach a Large Acene with Even-Number Linearly Fused Benzene Rings: 6,9,16,19-Tetraphenyl-1.20,4.5,10.11,14.15-Tetrabenzooctatwistacene. *J. Org. Chem.* **2015**, *80*, 109–113. (b) Kumarasinghe, K. G. U. R.; Fronczek, F. R.; Valle, H. U.; Sygula, A. Bis-corannuleno-anthracene: An Angularly Fused Pentacene as a Precursor for Barrelene-Tethered Receptors for Fullerene. *Org. Lett.* **2016**, *18*, 3054–3057.

(16) Duong, H. M.; Bendikov, M.; Steiger, D.; Zhang, Q.; Sonmez, G.; Yamada, J.; Wudl, F. Efficient Synthesis of a Novel, Twisted and Stable, Electroluminescent “Twistacene”. *Org. Lett.* **2003**, *5*, 4433–4436.

(17) (a) Wolthuis, E.; Cady, W. Reaction of Benzyne with α -Methylstyrene. *Angew. Chem., Int. Ed. Engl.* **1967**, *6*, 555–556. (b) Harrison, R.; Heaney, H.; Jablonski, J. M.; Mason, K. G.; Sketchley, J. M. Aryne Chemistry. Part XVIII. Some Reactions of Tetrahalogenobenzenes with Styrene and Substituted Styrenes. *J. Chem. Soc. C* **1969**, 1684–1689.

(18) (a) Dilling, W. L. The Reaction of Benzyne with Styrene. *Tetrahedron Lett.* **1966**, *7*, 939–941. (b) Bhojgude, S. S.; Bhunia, A.; Gonnade, R. G.; Biju, A. T. Efficient Synthesis of 9-Aryldihydrophenanthrenes by a Cascade Reaction Involving Arynes and Styrenes. *Org. Lett.* **2014**, *16*, 676–679. (c) Bhojgude, S. S.; Bhunia, A.; Biju, A. T. Employing Arynes in Diels-Alder Reactions and Transition-Metal-Free Multicomponent Coupling and Arylation Reactions. *Acc. Chem. Res.* **2016**, *49*, 1658–1670.

(19) Chen, Z.; Han, X.; Liang, J. H.; Yin, J.; Yu, G. A.; Liu, S. H. Cycloaddition Reactions of Benzyne with Olefins. *Chin. Chem. Lett.* **2014**, *25*, 1535–1539.

(20) See [Supporting Information](#) for details.

(21) In some experiments performed on a large scale, trace amounts of a monophenylated product were detected by mass spectrometry.

(22) Gross, L.; Mohn, F.; Moll, N.; Liljeroth, P.; Meyer, G. The Chemical Structure of a Molecule Resolved by Atomic Force Microscopy. *Science* **2009**, *325*, 1110–1114.

(23) (a) Gross, L.; Schuler, B.; Pavlicek, N.; Fatayer, S.; Majzik, Z.; Moll, N.; Peña, D.; Meyer, G. Atomic Force Microscopy for Molecular Structure Elucidation. *Angew. Chem., Int. Ed.* **2018**, *57*, 3888–3908 and references cited therein. (b) Peña, D.; Pavlicek, N.; Schuler, B.; Moll, N.; Pérez, D.; Guitián, E.; Meyer, G.; Gross, L. In *On-Surface Synthesis II. Advances in Atom and Single Molecule Machines*; de Oteyza, D., Rogero, C., Eds.; Springer: Cham, 2018; pp 209–227. (c) Fatayer, S.; Albrecht, F.; Zhang, Y.; Urbonas, D.; Peña, D.; Noll, N.; Gross, L. Molecular Structure Elucidation with Charge-State Control. *Science* **2019**, *365*, 142–145. (d) de Oteyza, D.

- G.; Gorman, P.; Chen, Y.-C.; Wickenburg, S.; Riss, A.; Mowbray, D. J.; Etkin, G.; Pedramrazi, Z.; Tsai, H.-Z.; Rubio, A.; Crommie, M. F.; Fischer, F. R. Direct Imaging of Covalent Bond Structure in Single-Molecule Chemical Reactions. *Science* **2013**, *340*, 1434–1437.
- (e) Rogers, C.; Chen, C.; Pedramrazi, Z.; Omrani, A. A.; Tsai, H.-Z.; Jung, H. S.; Lin, S.; Crommie, M. F.; Fischer, F. R. Closing the Nanographene Gap: Surface-Assisted Synthesis of Peripentacene from 6,6'-Bipentacene Precursors. *Angew. Chem., Int. Ed.* **2015**, *54*, 15143–15146.
- (f) Kawai, S.; Haapasilta, V.; Lindner, B. D.; Tahara, K.; Spijker, P.; Buitendijk, J. A.; Pawlak, R.; Meier, T.; Tobe, Y.; Foster, A. S.; Meyer, E. Thermal Control of Sequential On-Surface Transformation of a Hydrocarbon Molecule on a Copper Surface. *Nat. Commun.* **2016**, *7*, 12711.
- (g) Hieulle, J.; Carbonell-Sanromà, E.; Vilas-Varela, M.; García-Lekue, A.; Guitián, E.; Peña, D.; Pascual, J. I. On-Surface Route for Producing Planar Nanographenes with Azulene Moieties. *Nano Lett.* **2018**, *18*, 418–423.
- (h) Fan, Q.; Werner, S.; Tschakert, J.; Ebeling, D.; Schirmeisen, A.; Hilt, G.; Hieringer, W.; Gottfried, W. Precise Monoselective Aromatic C–H Bond Activation by Chemisorption of Meta-Aryne on a Metal Surface. *J. Am. Chem. Soc.* **2018**, *140*, 7526–7532.
- (i) Mishra, S.; Beyer, D.; Eimre, K.; Liu, J.; Berger, R.; Gröning, O.; Pignedoli, C. A.; Müllen, K.; Fasel, R.; Feng, X.; Ruffieux, P. Synthesis and Characterization of π -Extended Triangulene. *J. Am. Chem. Soc.* **2019**, *141*, 10621–10625.
- (j) Su, J.; Telychko, M.; Hu, P.; Macam, G.; Mutombo, P.; Zhang, H.; Bao, Y.; Cheng, F.; Huang, Z.-Q.; Qiu, Z.; Tan, S. J. R.; Lin, H.; Jelínek, P.; Chuang, F.-C.; Wu, J.; Lu, J. Atomically Precise Bottom-up Synthesis of π -Extended [5]Triangulene. *Sci. Adv.* **2019**, *5*, No. eaav7717.
- (k) Sánchez-Grande, A.; de la Torre, B.; Santos, J.; Cirera, B.; Lauwaet, K.; Chutora, T.; Edalatmanesh, S.; Mutombo, P.; Rosen, J.; Zbořil, R.; Miranda, R.; Björk, J.; Jelínek, P.; Martín, N.; Écija, D. On-Surface Synthesis of Ethynylene-Bridged Anthracene Polymers. *Angew. Chem., Int. Ed.* **2019**, *58*, 6559–6563.
- (24) (a) Rapenne, G.; Grill, L.; Zambelli, T.; Stojkovic, S. M.; Ample, F.; Moresco, F.; Joachim, C. Launching and Landing Single Molecular Wheelbarrows on a Cu (100) Surface. *Chem. Phys. Lett.* **2006**, *431*, 219–222. (b) Schuler, B.; Meyer, G.; Peña, D.; Mullins, O. C.; Gross, L. Unraveling the Molecular Structures of Asphaltenes by Atomic Force Microscopy. *J. Am. Chem. Soc.* **2015**, *137*, 9870–9876.
- (25) Gross, L.; Mohn, F.; Moll, N.; Meyer, G.; Ebel, R.; Abdel-Mageed, W. M.; Jaspars, M. Organic Structure Determination Using Atomic Resolution Scanning Probe Microscopy. *Nat. Chem.* **2010**, *2*, 821–825.
- (26) Bartels, L.; Meyer, G.; Rieder, K. H. Controlled Vertical Manipulation of Single CO Molecules with the Scanning Tunneling Microscope: A Route to Chemical Contrast. *Appl. Phys. Lett.* **1997**, *71*, 213–215.
- (27) Gross, L.; Mohn, F.; Moll, N.; Schuler, B.; Criado, A.; Guitin, E.; Peña, D.; Gourdon, A.; Meyer, G. Bond-Order Discrimination by Atomic Force Microscopy. *Science* **2012**, *337*, 1326–1329.
- (28) Hapala, P.; Kichin, G.; Wagner, C.; Tautz, F. S.; Temirov, R.; Jelínek, P. Mechanism of High-Resolution STM/AFM Imaging with Functionalized Tips. *Phys. Rev. B: Condens. Matter Mater. Phys.* **2014**, *90*, 085421.
- (29) Majzik, Z.; Pavliček, N.; Vilas-Varela, M.; Pérez, D.; Moll, N.; Guitián, E.; Meyer, G.; Peña, D.; Gross, L. Studying an Antiaromatic Polycyclic Hydrocarbon Adsorbed on Different Surfaces. *Nat. Commun.* **2018**, *9*, 1198.
- (30) This level of calculations has been found to reproduce quantitatively key electronic properties of other PAHs, for instance: (a) Cortizo-Lacalle, D.; Mora-Fuentes, J. P.; Strutynski, K.; Saeki, A.; Melle-Franco, M.; Mateo-Alonso, A. Monodisperse N-Doped Graphene Nanoribbons Reaching 7.7 Nanometers in Length. *Angew. Chem., Int. Ed.* **2018**, *57*, 703–708. (b) Marco, A. B.; Cortizo-Lacalle, D.; Gozalvez, C.; Olano, M.; Atxabal, A.; Sun, X.; Melle-Franco, M.; Hueso, L. E.; Mateo-Alonso, A. An Electron-Conducting Pyrene-Fused Phenazinothiadiazole. *Chem. Commun.* **2015**, *51*, 10754–10757.
- (31) (a) Clar, E. *The Aromatic Sextet*; Wiley: New York, 1972. (b) Solá, M. Forty Years of Clar's Aromatic π -Sextet Rule. *Front. Chem.* **2013**, *1*, 22.
- (32) Hapala, P.; Temirov, R.; Tautz, F. S.; Jelínek, P. Origin of High-Resolution IETS-STM Images of Organic Molecules with Functionalized Tips. *Phys. Rev. Lett.* **2014**, *113*, 226101.
- (33) Similar to previous findings: (a) Ellner, M.; Pavliček, N.; Pou, P.; Schuler, B.; Moll, N.; Meyer, G.; Gross, L.; Pérez, R. The Electric Field of CO Tips and Its Relevance for Atomic Force Microscopy. *Nano Lett.* **2016**, *16*, 1974–1980. (b) Hapala, P.; Svec, M.; Stetsovych, O.; van der Heijden, N. J.; Ondracek, M.; van der Lit, J.; Mutombo, P.; Swart, I.; Jelínek, P. Mapping the Electrostatic Force Field of Single Molecules from High-Resolution Scanning Probe Images. *Nat. Commun.* **2016**, *7*, 11560.
- (34) For values of the measured and simulated apparent bond lengths, see [Supporting Information](#).